IMPORTANCE OF POROUS PLATE MEASUREMENTS ON CARBONATES AT PSEUDO RESERVOIR CONDITIONS

M Z Kalam[1], K Al Hammadi[1], O B Wilson[2], M Dernaika[2] and H Samosir[2]
Abu Dhabi Company for Onshore Oil Operations[1] and ResLab AS[2]

This paper was prepared for presentation at the International Symposium of the Society of Core Analysts held in Trondheim, Norway 12-16 September, 2006

ABSTRACT

Porous plate method (PP) has been used for years in acquiring reliable capillary pressure (Pc) data, representative of reservoir rock-fluid properties. In recent years, the method is also found to be reliable and subject to less experimental errors and analysis when used for electrical resistivity (RI) measurements as well. A major problem has been the long time scales required for achieving reliable data. This work describes the recent advances made in water-oil capillary pressure measurements in carbonates, that is fundamental to consistent and reliable static models in reservoir engineering. A coherent S_w-RI measurement is the basis of defining reservoir fluid saturations accurately and in validating logs used to interpret these saturations.

The study focused on acquiring reliable and consistent water-oil Pc and S_w-RI measurements on carbonate reservoir cores using a variety of techniques including Porous Plate method, Continuous Injection technique (CI), Centrifuge and Fast Resistivity Index Measurements (FRIM). More than 70 reservoir cores, comprising four different carbonate reservoirs are investigated. The pitfalls of each technique is discussed with the data examined, and a rigorous development of PP is presented to capture the important primary drainage, spontaneous imbibition and forced imbibition cycles at reservoir stress conditions and reservoir temperature.

A robust error analysis and possible uncertainty in laboratory measurements is presented to minimize risks associated with SCAL data. The impact of reliable water-oil Pc and S_w-RI data is shown from an analysis of STOOIP and static model developed in a typical carbonate reservoir.

INTRODUCTION

The determination of representative capillary pressure curves and S_w-RI relationships is of vital importance for the mapping of reservoir fluid distribution. The most frequently used techniques today are centrifugation, porous plate method, mercury injection, continuous injection, FRIM and very limited measurements using the semi-dynamic method, see Lombard et al, (2002). Key features of these techniques are briefly discussed and summarised.

The Porous Plate Technique

The principle of the porous plate technique [see Longeron et al. (1989), Wilson et al. (2001) and Wilson and Skjaeveland (2002)] is to invade a water saturated core plug with a non-wetting fluid by applying a constant displacement pressure stepwise towards irreducible water saturation. The porous ceramic plate is coupled in series with the water saturated porous medium, like a composite core. The traditional porous plate technique is very reliable but quite time consuming. The aim of the porous plate is to prevent the non-wetting phase to break through the barrier, i.e. the porous plate, at all stages of the experiment. This will not happen as long as the capillary pressure is kept below the entry pressure of the ceramic plate. For incrementally higher pressures, the non-wetting phase will enter the water saturated ceramic plate and the experiment has to be terminated.

The strength of the porous plate technique is the possibility to establish primary drainage, spontaneous imbibition, forced imbibition and secondary drainage without changing set up, conditions or method. Further, uniform saturations mimicking typical distribution of fluids in reservoir rocks (porous media) is one of its best advantages. The method has been used under different conditions since the late eighties. If a full cycle curve is required, a hydrophobic version of the ceramic porous plate needs to be mounted in the opposite end of the core plug. The reason for this is to prevent the water breaking through during all stages of forced imbibition.

One reason for the popularity of the technique is the possibility to combine experimental capillary pressure curves with other measurements such as resistivity index or nuclear magnetic resonance (NMR) measurements. In addition, hierarchies and mechanisms developing as a function of saturation history are controlled by capillary forces in the system. This is the main reason why drainage and imbibition data from porous plate technique are popular in history matching core flooding experiment.

The disadvantage is that it is very time consuming. A reliable and representative full cycle capillary pressure curve might take as long as 12-18 months in carbonates. Due to its established reliability and consistency over the years, all other capillary pressure techniques use the porous plate technique as a reference in comparison studies.

The Continuous Injection Technique

In the early nineties, the continuous injection technique [see Zeelenberg and Schipper (1991), Kokkede and Maas (1994) and Maas and Van der Post (2000)] was introduced to the industry as a fast and reliable replacement technique for the porous plate technique. This technique is identical to the traditional porous plate technique except that the experiment is performed using an ultra low constant injection or withdrawal rate instead of using a stepwise constant differential pressure.

When the continuous injection technique was introduced to the industry, it was well accepted. One of the reasons for this is that it frequently showed curved S_w-RI

relationships instead of linear relationships, which is often observed for equilibrium data from porous plate technique. It was reported by Kokkede and Maas (1994) to have the potential for measuring reliable capillary pressure curves simultaneously with reliable and representative S_w-RI relationships. In addition, it was suggested that the method could be used to simultaneously establish representative relative permeability curves.

The Centrifuge Technique

The principle of the centrifuge technique is to invade water saturated core plug with a non-wetting fluid by centrifuging. The method is indirect and depends on models to calculate water saturation. The saturation distribution is non-uniform due to end-effects, which need to be taken care of by the assumed model and possible numerical simulations. The differential pressure across the core plug is calculated from the rotational speed at all stages. The reason for the popularity of this method is the fast turn around time of the experiment. The disadvantage of the method is that it is impossible to obtain spontaneous imbibition or spontaneous re-drainage by centrifuging. In addition, maintaining plug integrity might be questionable in some cases due to the force acting on the grains while centrifuging. It is also difficult to combine the technique with electrical measurements such as resistivity index measurements. In addition, the technique is not suitable for weakly or unconsolidated core material.

Fast Resistivity Index Measurements

FRIM [see Fleury (2000) and Fleury and Longeron (1997)] was introduced to the industry as a fast and reliable replacement technique for the continuous injection technique. This technique is identical to the traditional porous plate technique except that the experiment is performed with a relatively high constant differential pressure in order to experimentally describe first time invasion in few days. The strength of the technique is that it is standardised with direct individual 4-wire electrode assembly. The technique has the advantage of avoiding the possibility that viscous forces can dominate and influence regime development. On the other hand, there might be a saturation profile in the plug, caused by the high displacement pressure, resulting in abnormal S_w-RI relationship, i.e. an end-effect.

COMPARISON STUDY

A comparison study for establishing representative capillary and electrical properties, from different Petrophysical experimental methods on core plugs from four different Carbonate fields in the Middle East, has been investigated. Porous plate method was used on selected core plugs from all four reservoirs as a reference method. In parallel with this, continuous injection experiments were investigated on selected core plugs from field B, while FRIM experiments were investigated on selected core plugs from field D. All experiments were performed at pseudo reservoir conditions, i.e. dead crude oil-brine systems at net effective reservoir stress and reservoir temperature.

In Tables 1-5, RRT is for reservoir rock type, phi is fractional porosity, NOP is net overburden pressure, FF is formation resistivity factor, atm is atmospheric pressure, m is cementation exponent, Kw is brine permeability, Swi is irreducible water saturation, n is saturation exponent, Sor is residual oil saturation, WI is wettability index and USBM is US Bureau of Mines. Further, drainage is used for defining a situation where oil is injected to displace brine, and conversely imbibition is used when brine is injected to displace oil.

Field A

Porous plate derived properties for Field A, presented in Table 1 and Figure 1, show one distinct dimensionless capillary pattern within the field. An average saturation exponent of 2.14 with a standard deviation of 0.104 is achieved. Furthermore, wettability index from porous plate measurements indicate a mixed system near neutral wettability.

Field B

Porous plate derived properties for field B, presented in Table 2 and Figure 2, show one distinct dimensionless capillary pattern for the field. Experiment no. 5 deviates with this observation due to an abnormal high permeability. An average saturation exponent of 2.47 with a standard deviation of 0.299 is achieved, indicating a moderate variance in n-exponent within the field.

Table 3 and Figure 3 refer to Continuous Injection data for field B. It is observed that achieved water saturation at injection (during primary drainage cycle) stop at much higher brine saturation compared with the porous plate method. Furthermore, an average saturation exponent of 2.16 with a standard deviation of 0.910 is achieved. The large variation in continuous injection derived n-exponent indicates that it is impossible to determine a reliable average n-exponent for use in log interpretation without having porous plate method derived n-exponents. The impact of decreasing the saturation exponent from 2.47 to 2.16 is quite significant for the saturation interpretation and consequently on the STOOIP.

Field C

Porous plate derived properties for field C, presented in Figure 4, shows one distinct dimensionless capillary pattern for the field. An average saturation exponent of 2.16 with a standard deviation of 0.094 is achieved.

Field D

Porous plate derived properties for field D, presented in Table 4 and Figure 5, show that there exist several distinct dimensionless capillary patterns for the field. The porous plate measurements indicate that electrical properties for the seven classified rock types in the field is properly described by two n-exponents. An average saturation exponent of 1.99 with a standard deviation of 0.160 is achieved for rock type 1-5. An average saturation exponent of 1.61 with a standard deviation of 0.161 is achieved for rock type 6-7.

By adding Table 5 and Figure 6 into the interpretation, it is observed that pseudo capillary pressure curves from FRIM technique deviates with porous plate derived behaviour. However, low brine saturations obtained match well with corresponding porous plate results.

Derived S_w-RI relationship from FRIM method deviates from usual linear approximations. An average saturation exponent of 1.80 with a standard deviation of 0.252 is reported. A non-linear S_w-RI relationship is observed in some of the samples despite absence of any micro-porosity and obvious local heterogeneity. The large variation in FRIM derived n-exponent, points towards impossible to determine and reliable n-exponent from FRIM method without having porous plate experiments for comparison. The numbers for each curve represents the different rock types analysed. The upward and downward bends were not consistent with any measured permeability or wettability trends. Such behaviour is not observed in any of the corresponding porous plate measurements, reported in Figure 5. More importantly, porous plate derived measurements were repeatable on similar rock type samples. Further, in reproduced tests on samples from same RRT, similar trends were not observed using FRIM. Hence, the impact of uncertain saturation exponent values during both drainage and imbibition using FRIM is considerable when evaluating STOOIP.

EXPLORING DATA BY PRINCIPAL COMPONENT ANALYSIS

In order to reduce uncertainty when implementing the experimental results in the formation evaluation process, it is important to explore, detect and possibly remove outliers within the experimental data matrix.

Principal component analysis (PCA) [see Birks (1987) and Kvalheim (1988)] is a multivariate technique that finds orthogonal linear combinations in a data matrix, with the additional purpose of minimizing the residual variance of a data matrix. The first principal component, PC1, is the linear combination with maximal variation, i.e. a dimension along which the observations display the highest degree of separation or diversity. The second principal component, PC2, is the linear combination with maximal variance in a direction orthogonal to the first principal component. The third principal component, PC3, is equally orthogonal to the first and the second principal component.

Score plots show the position of the objects, i.e. experiments, when being projected onto the plane spanned by the components. Similarities between core plugs are quantified in terms of internal distances and angle. Loading plots display the latent variable of the data matrix, i.e. a linear combination of the measured properties. The contribution from each property on a latent variable of the data matrix is explained by its positioning. Biplots are a display of the position of variables and objects. Angles between a pair of variables and between a pair of objects show the degree of correlation and similarity respectively. Leverage plot illustrates the how much each object influence the PCA model and how much of this is unexplained variance (residual variance)

Interpretation of PCA Analysis

The percentages represent total experimental variance. Thus 91 % of the total experimental variance has been captured by analyzing principal component number 1-3. The score plots, summarized in the 3-D score plot presented in Figure 7a, detects experiment P19 and P26 from Field B, and P40 and P57 from Field D as outliers. In other words, the dimensionless pattern for these core plugs does not fit the general dimensionless pattern for respective Fields.

By analyzing PC1 versus PC2, i.e. considering 79.5 % of the total static variance presented in Figure 7b, it seems that data from field A and D fits one linear multivariate variance model. This indicates similarities between the two fields. In addition, the multivariate linearity indicates consistency in variance. It is also observed that Field B is much more scattered than the other fields. The scattered behaviour for this Field is not captured by adding one more principal component, i.e. PC3, to the interpretation. This can be seen in Figure 7d where Field B data more and less fits an internal circle inside the statistical accept criteria, i.e. 0.05 in significance level.

Analyzing Biplots, presented in Figure 8a-c, reveals that all four detected outliers are taken out by the variable irreducible water saturation. The borderline objects P27 and P56 indicates that the pattern between Swi and m-exponent versus n-exponent is different compared with the general pattern detected. By borderline object it means that the object is near the borderline of acceptable criteria. Figure 8c indicates that the observed scattered behaviour for Field B is caused by the variance in n-exponent within the Field. It also suggests that Field C is more and less described by a linear multivariate variance model which is parallel to the model for Field A and D. Experiment P34 deviates from this observation.

By analyzing the Leverage plot and the influence of variable to total variation plot, presented in Figures 9a and 9b, it reveals that the largest contribution to unexplained variance is variance in irreducible water saturation, then formation resistivity factor. The Leverage plot, presented in Figure 9a, indicates that P19, P26, P40 and P47 have a massive impact on the total variance. In addition, most of this variance is unexplained.

CONCLUSIONS AND RECOMMENDATIONS

Porous Plate technique offers robust and dependable acquisition of water-oil capillary pressure (Pc) and resistivity indices (Sw-RI) at reservoir temperature and reservoir overburden pressures with dead crude oil and simulated formation brine. The repeatability and confidence in the measured data is reflected during both primary drainage and imbibition cycles.

Principal Component Analysis has been found to be a useful tool for statistically identifying the outliers, analyzing the reason for this and check consistency in the SCAL measurements before it is implemented in the formation evaluation process.

The primary drainage tests on the 76 reservoir core plugs from four carbonate reservoirs confirm the validity of the porous plate method for both Pc and n-exponent, and show the uncertainty and experimental errors observed on comparable tests with Continuous Injection and Fast Resistivity Injection Measurements.

The validity of these tests at full reservoir conditions with live crude is yet to be explored although initial measurements show gross uncertainty of data at full reservoir conditions.

ACKNOWLEDGEMENTS

The authors wish to acknowledge ADNOC and ADCO Management for permission to publish the results of the various SCAL studies entailed in this paper.

REFERENCES

Birks HJB (1987),"Multivariate Data Analysis in Geology and Geochemistry: An Introduction", Chemometrics and Intelligent Laboratory Systems 2 (1987) 15-28.

Fleury M and Longeron DG (1997),"Full Imbibition Capillary Pressure Measurements On Preserved Samples Using The Membrane Technique", SCA 9716 – Calgary, Canada.

Fleury M (2000),"FRIM - A New Method For Measuring Continuous Resistivity Index Curves" SCA 2000 - Abu Dhabi, UAE.

Kokkede J and Maas J (1994),"Capillary Pressure, Relative Permeability And Resistivity Index By Continuous Injection", 3rd International Symposium On Evaluation Of Wettability And Its Effect On Oil Recovery, Laramie, Wyoming 1994.

Kvalheim OM (1988),"Interpretation Of Direct Latent-variable Projection Methods And Their Aims and Use in Analysis of Multi-component Spectroscopic and Chromatographic Data", Chemometrics and Intelligent Laboratory System, 4 (1988) 11-25.

Lombard JM, Egermann P and Lenormand R (2002),"Measurement Of Capillary Pressure Curves at Reservoir Conditions", SCA 2002 – Monterey, USA

Longeron DG, Arquad MJ and Bouvier L (1989),"Resistivity Index And Capillary Pressure Measurements Under Reservoir Conditions", SPE 19589, San Antonio, USA.

Maas J and Van der Post N (2000),"Resistivity Index Measurements Under Weak Capillary Forces", SCA 2000 - Abu Dhabi, UAE.

Wilson OB, Tjetland BG and Skauge A (2001),"Porous Plate Influence On Effective Drainage Rates In Capillary Pressure Experiments" SCA 2001- Edinburgh, Scotland.

Wilson OB and Skjæveland SM (2002),"Porous Plate Influence On Effective Imbibition Rates In Capillary Pressure Experiments" SCA 2002 – Monterey, USA.

Zeelenberg HPW and Schipper BA (1991),"Developments In I-Sw measurements" Advances In Core Evaluation 2, Gordon and Breach Science Publishers 1991.

Table 1 Porous plate data (Field A)

RRT	Plug no	Φ NOP (frac.)	FF atm	m NOP	Kw atm (mD)	Swi NOP (frac.)	n NOP drainage	Sor NOP (frac.)	n NOP Imbibition	WI NOP Modified USBM
1	G	0.130	45.22	1.95	0.22	0.103	1.94	0.207	2.04	0.17
1	N	0.145	35.65	1.89	0.65	0.134	2.10	0.204	1.95	0.02
1	Q	0.207	19.84	1.95	3.19	0.061	2.13	0.212	1.95	0.32
1	66	0.189	19.64	1.83	1.38	0.054	2.20	0.220	2.28	-0.05
1	EE	0.161	27.45	1.88	0.31	0.111	2.16	0.246	2.04	0.11
2	C	0.176	25.21	1.94	0.48	0.076	2.02	0.196	2.22	0.18
2	I	0.231	16.05	1.93	3.89	0.057	2.26	0.193	2.12	0.10
2	51	0.201	18.30	1.85	1.50	0.062	2.19	0.225	2.15	-0.02
2	63	0.205	20.06	1.94	0.86	0.077	2.19	0.211	2.15	-0.02
2	73	0.217	18.80	1.98	2.56	0.077	2.21	0.220	2.28	-0.08
2	81	0.161	28.20	1.85	0.41	0.083	2.20	0.205	2.20	-0.06
3	F	0.180	25.74	1.95	1.86	0.062	1.93	0.238	2.21	0.38
3	8	0.182	29.91	2.06	1.80	0.067	1.97	0.246	2.20	0.34
3	L	0.205	18.11	1.87	2.29	0.103	2.20	0.239	2.23	-0.07
3	24	0.251	12.61	1.86	4.35	0.044	2.10	0.223	2.17	0.29
3	46	0.213	19.51	1.96	1.43	0.071	2.24	0.244	2.20	0.08
3	82	0.187	21.60	1.86	0.72	0.061	2.19	0.247	2.18	0.13
3	89	0.211	17.95	1.88	3.06	0.048	2.21	0.242	2.22	-0.06

Table 2 Porous Plate data (Field B)

Plug no	Φ NOP (frac.)	m NOP	Kw atm (mD)	Swi NOP (frac.)	n NOP drainage
1	0.090	1.97	0.04	0.523	1.87
2	0.184	1.73	2.3	0.043	2.35
3	0.206	1.80	2.9	0.052	2.21
4	0.190	1.81	2.3	0.068	2.76
5	0.196	1.92	1998	0.128	2.06
6	0.208	1.89	5.4	0.078	2.71
7	0.180	1.83	3.3	0.080	2.61
8	0.069	1.97	0.03	0.360	2.36
9	0.109	2.07	0.15	0.243	2.23

Table 3 Continuous Injection data (Field B)

Plug no	Φ NOP (frac.)	m NOP	Kw atm (mD)	Swi NOP (frac.)	n NOP drainage	Sor NOP (frac.)	n NOP Imbibition free fit	n NOP Imbibition forced fit
12	0.195	2.46	2.35	0.276	2.19	0.129	1.51	2.97
35D	0.236	2.20	2.7	0.200	1.91			
37B	0.214	2.16	2.9	0.350	2.26			
38B	0.216	2.07	3.5	0.675	4.21			
47B	0.155	2.05	0.53	0.330	1.90	0.211	1.33	2.94
113A	0.162	1.75	0.80	0.400	2.01			
113B	0.165	1.83	1	0.400	2.12	0.137	1.04	2.98
38C	0.209	1.77	6.8	0.425	2.65			
42	0.207	1.76	5.2	0.575	4.22			
51B	0.161	1.95	2.1	0.345	1.90	0.218	1.60	3.16

Table 4 Porous Plate data (Field D)

RRT	Plug no	Φ atm frac.	Kw atm	Swi NOP	n NOP drainage
1	5	0.268	5336	0.131	2.12
1	B	0.275	633	0.055	1.85
2	9	0.323	164	0.069	2.08
2	15	0.342	223	0.061	2.09
2	18	0.301	240	0.053	1.88
3	8	0.320	30	0.068	2.06
3	16	0.327	42	0.057	2.07
3	19	0.349	59	0.045	1.91
4	22	0.275	23	0.065	1.98
4	32	0.296	9.1	0.054	1.97
4	33	0.267	7.1	0.044	1.87
5	1	0.230	2.2	0.101	1.82
5	34	0.226	2.9	0.091	2.15
5	41	0.130	1.8	0.181	1.55
6	2	0.168	0.80	0.146	1.72
6	39	0.140	0.36	0.111	1.75
6	43	0.166	0.37	0.14	1.54
7	40	0.112	0.02	0.118	1.41

Table 5 FRIM data (Field D)

RRT	Plug no	Φ atm frac.	Kw atm	Swi NOP (frac.)	n NOP drainage
1	306	0.261	1428	0.050	1.50
1	409	0.298	1994	0.060	1.50
2	408	0.221	330	0.150	1.85
2	34	0.239	437	0.100	1.85
3	309	0.347	49	0.180	2.05
3	43	0.345	32	0.100	2.05
4	307	0.345	12	0.100	1.50
4	42	0.289	22	0.020	1.50
4	119	0.314	6.1	0.030	1.50
4	121	0.288	5.1	0.060	1.50
5	172	0.306	3.7	0.030	1.50
5	85	0.341	2.7	0.070	2.10
6	183	0.206	0.5	0.080	1.70
7	204	0.152	0.08	0.350	2.00

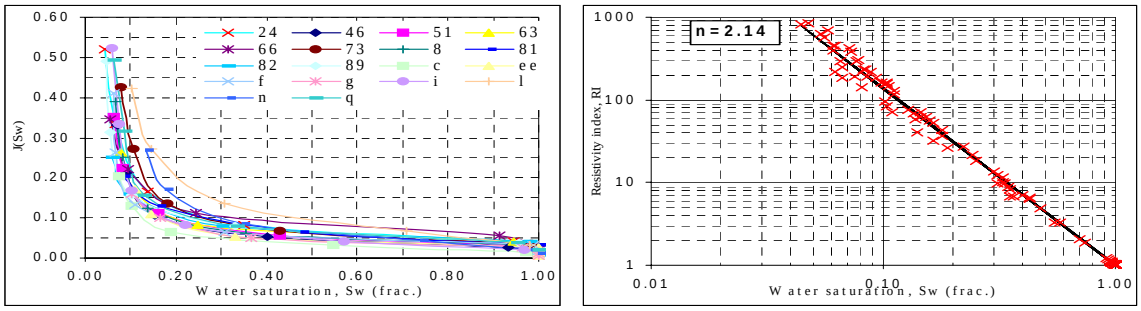

Figure 1 Capillary and electrical properties from porous plate method, Field A

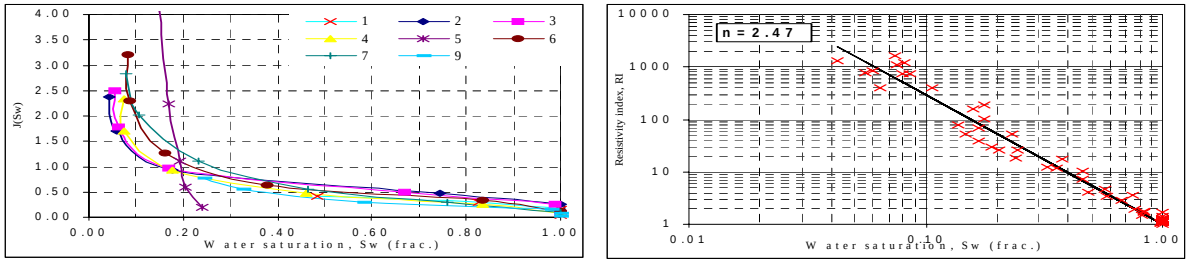

Figure 2 Capillary and electrical properties from porous plate method, Field B

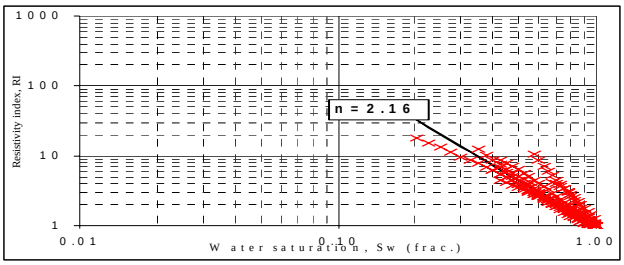

Figure 3 Sw-RI relationships by continuous injection technique, Field B.

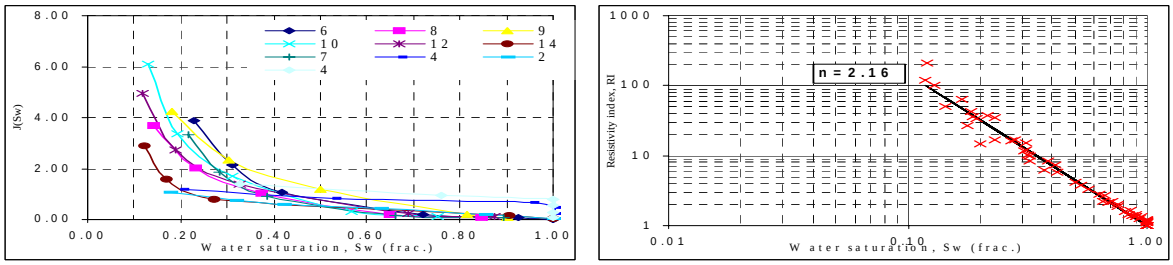

Figure 4 Capillary and electrical properties from porous plate method, Field C

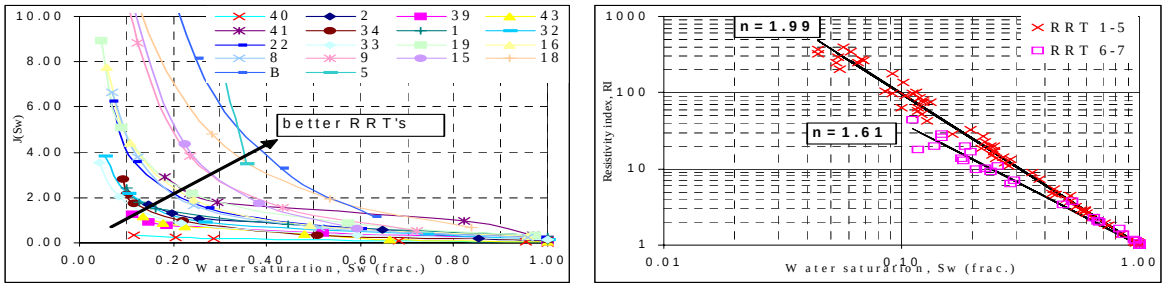

Figure 5 Capillary and electrical properties from porous plate method, Field D

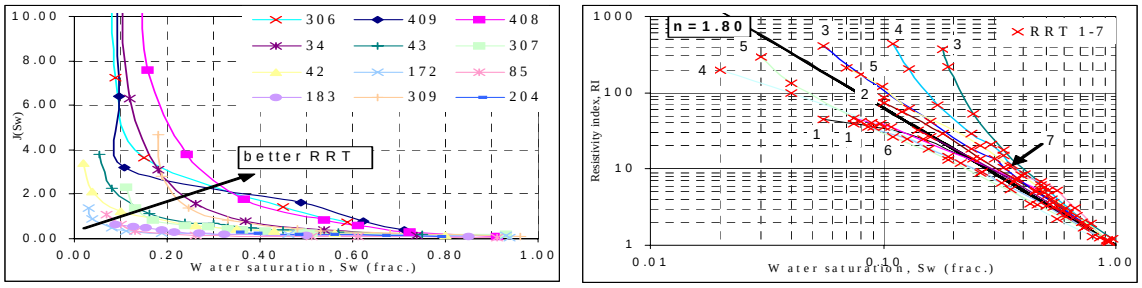

Figure 6 Capillary and electrical properties from FRIM method, Field D

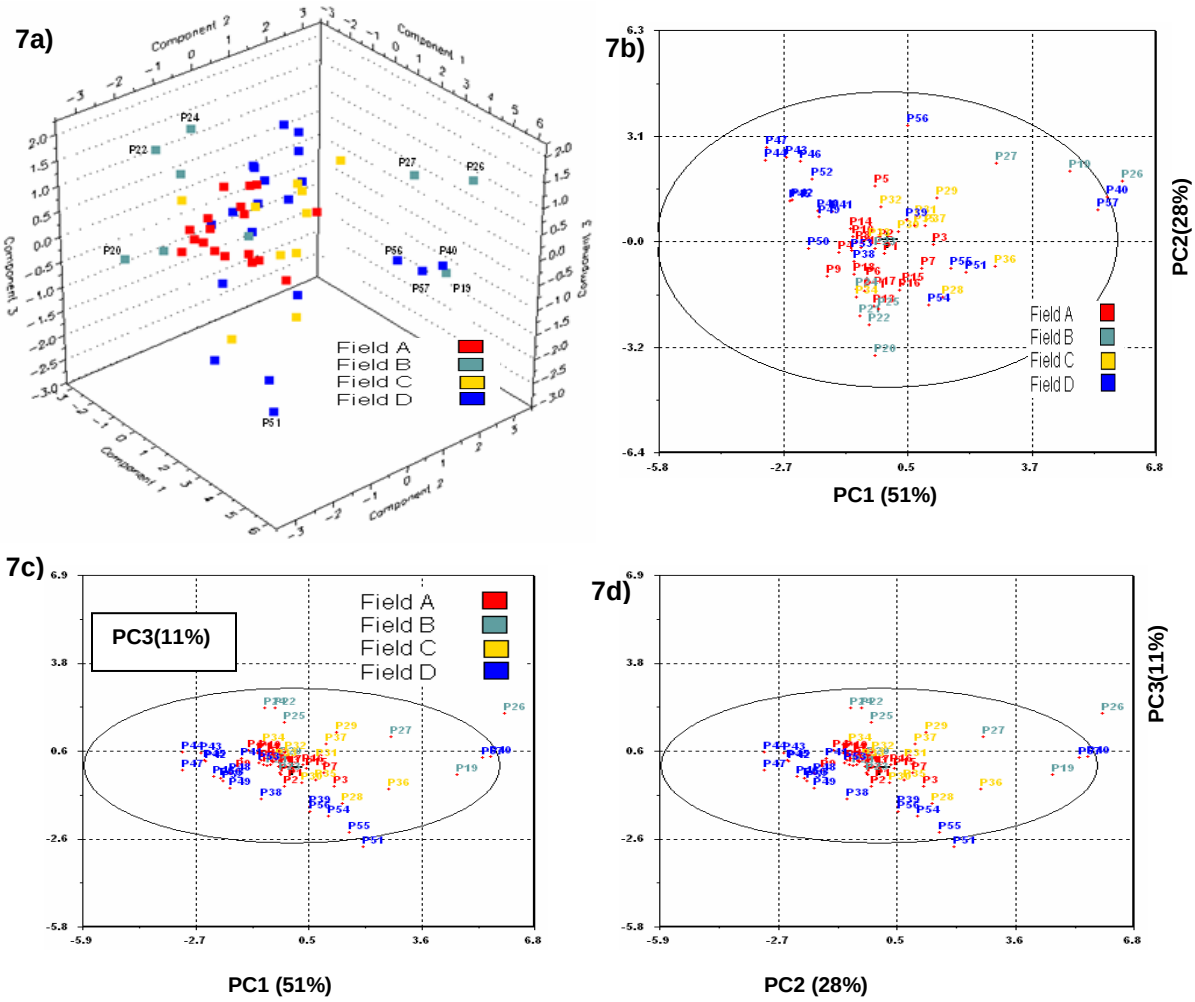

Figure 7: a. 3-D score plot; b. Score plot PC1 vs. PC2; c. Score plot PC1 vs. PC3; d. Score plot PC2 vs. PC3.

In the above figures, PC1 (51%) refers to 51 percent total experimental variance with respect to principal component 1, PC2 (28%) means 28 percent total experimental variance with respect to principal component 2, and similarly PC3 (11%) is 11 percent total experimental variance in principal component 3.

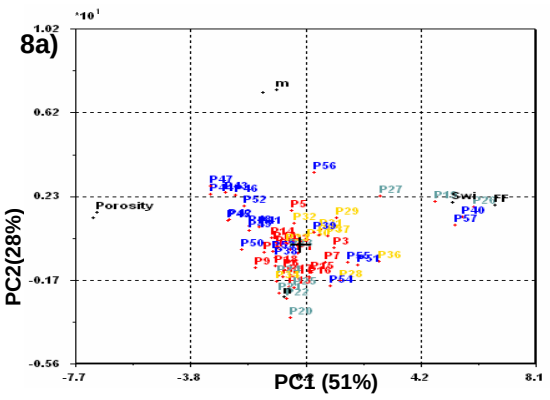

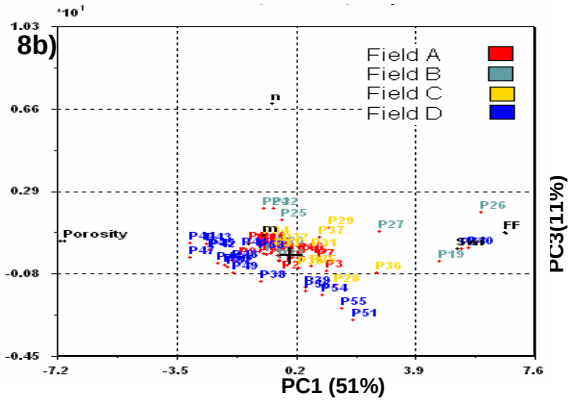

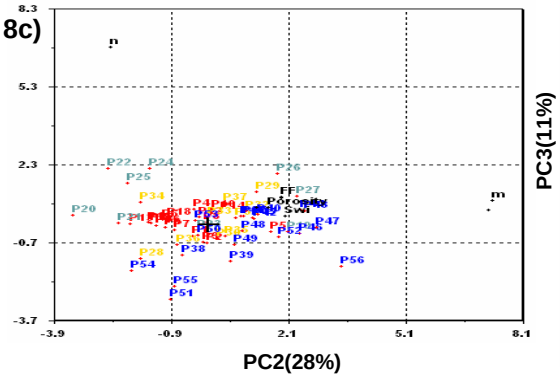

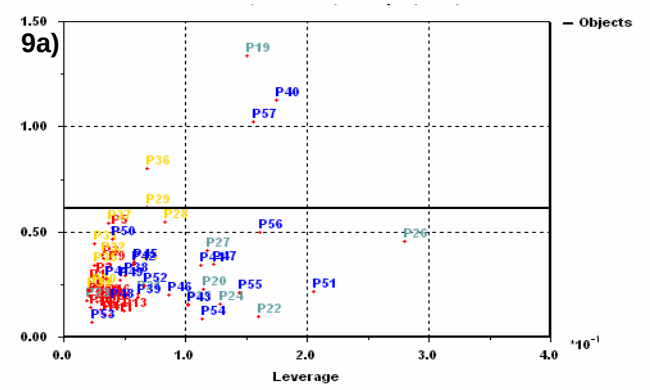

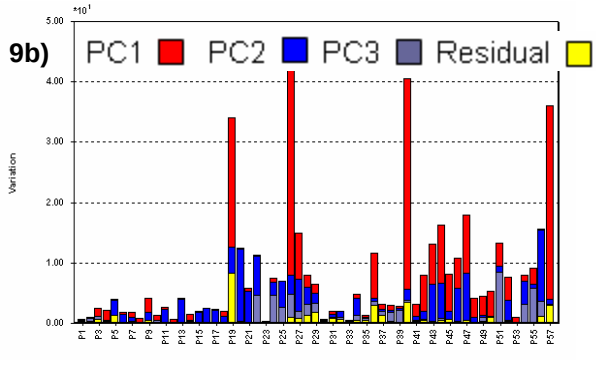

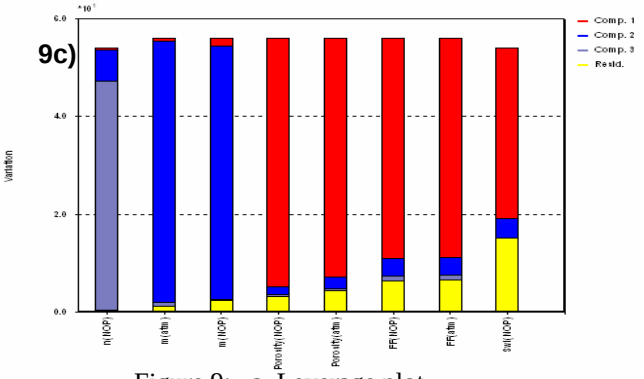

Figure 8: a. Biplot PC1 vs. PC2
b. Biplot PC1 vs. PC3
c. Biplot PC2 vs. PC3.

Figure 9: a. Leverage plot
b. Object variation
c. Variable variation plot